PHYSICAL REVIEW E **85**, 045301(R) (2012)

Preasymptotic hydrodynamic dispersion as a quantitative probe of permeability

Tyler R. Brosten,[1,*] Sarah J. Vogt,[2] Joseph D. Seymour,[2] Sarah L. Codd,[3] and Robert S. Maier[1]
[1]*U.S. Army Engineer Research and Development Center, 3909 Halls Ferry Road, Vicksburg, Mississippi 39180-6199, USA*
[2]*Department of Chemical and Biological Engineering, Montana State University, Bozeman, Montana 59717-3920, USA*
[3]*Department of Mechanical and Industrial Engineering, Montana State University, Bozeman, Montana 59717-3920, USA*
(Received 28 October 2011; published 5 April 2012)

We interpret a generalized short-time expansion of stochastic hydrodynamic dispersion dynamics in the case of small Reynolds number flow through macroscopically homogenous permeable porous media to directly determine hydrodynamic permeability. The approach allows determination of hydrodynamic permeability from pulsed field gradient spin-echo nuclear magnetic resonance measurement of the short-time effective hydrodynamic dispersion coefficient. The analytical expansion of asymptotic dynamics agrees with experimental NMR data and lattice Boltzmann simulation of hydrodynamic dispersion in consolidated random sphere pack media.

DOI: 10.1103/PhysRevE.85.045301 PACS number(s): 47.56.+r, 81.05.Rm

Macrotransport models that evolve from pore-scale dynamics in porous media have implications across the physical and life sciences [1]. The common pore-scale scenario of steady fluid flow dominated by viscous forces is modeled on the macro scale by Darcy's law [1–3], $\varepsilon\mu\bar{\mathbf{u}} = \mathbf{k}\,(\mathbf{f} - \nabla\bar{p})$. Macroscopically homogenous (MH) porous media [4] are characterized by a spatially uniform fluid volume fraction ε and permeability tensor $\mathbf{k}$ that couple the intrinsic volume-average saturating fluid velocity $\bar{\mathbf{u}}$, dynamic fluid viscosity μ, gradient of the intrinsic average fluid pressure $\nabla\bar{p}$, and body force $\mathbf{f}$. Connection of pore geometry and permeability is an outstanding question, and complex pore structures necessitate a measurement of permeability [1–3]. Estimates of permeability govern environmental, engineering, and economic models used in the management of groundwater and petroleum resources, design of novel flow control [5], and study of physiological fluid transport [6].

In this Rapid Communication we demonstrate the connection between permeability and a short-time expansion of ensemble average hydrodynamic dispersion dynamics resulting from Stokes flow through MH porous media. The connection is made through the interaction of molecular diffusion and a mechanical potential gradient, with fluid pressure being only one of the possible potentials. The result facilitates a noninvasive measurement of permeability by a postprocessing pulsed field gradient spin-echo (PGSE) nuclear magnetic resonance (NMR) measurement of the relevant dynamics. In the following, we first present the final results of a generalized short-time expansion of the effective dispersion coefficient and reduction in the case of Stokes flow through MH porous media, demonstrating that the coefficient scales with permeability. We then outline the derivation in detail. Finally, the ansatz is compared with numerical random-walk particle tracking transport simulation in consolidated random sphere pack media and experimental PGSE NMR data.

The approach is restricted to Stokes flow, defined here as pressure-driven, steady, Newtonian, single-phase, incompressible, small Reynolds number flow $\mathrm{Re} = uL\rho/\mu \ll 1$, where L is the characteristic pore-length scale, u is the mean flow velocity, and ρ is the fluid density. The fluid is assumed to fully saturate the pore volume of an equilibrated MH porous media that is bounded by a rigid, reflecting (i.e., the fluid tracer particles are conserved), no-slip, and piecewise-smooth (i.e., finite surface curvature and nonfractal) pore-grain interface. As will be later shown, these constraints, when applied to the general short-time expansion of the time t-dependent effective dispersion coefficient $D(t) = \langle|\mathbf{R}(t) - \langle\mathbf{R}(t)\rangle|^2\rangle/6t$ of fluid particle displacement $\mathbf{R}(t)$, imply $D(t)$ varies as

$$D(t) = D_o(t) + \frac{1}{6}\overline{\mathbf{u}'\cdot\mathbf{u}'}\,t - \frac{u^2\varepsilon\kappa}{18k}t^2 + O(t^{5/2}) \qquad (1)$$

as $t\to 0^+$. Here the brackets and overbar denote ensemble and pore-volume average, respectively, the mean flow velocity is $u = |\bar{\mathbf{u}}|$, κ is the molecular diffusion constant, $D_o(t)$ is $D(t)$ without convection, and $k = \varepsilon\mu u/|\mathbf{f} - \nabla\bar{p}|\cos\theta$ is directional permeability in the direction of the flow [1–3], where θ is the angle between $\bar{\mathbf{u}}$ and the hydraulic gradient. At short times $D_o(t) = \kappa - A_o(\kappa^3 t)^{1/2} + O(t)$, where A_o is governed by the surface area to pore-volume ratio [7,8]. Equation (1) with the Green-Kubo relation [9] $D(t) = D_o(t) + (3t)^{-1}\int(t-t')\psi(t')dt'$ implies the velocity autocorrelation $\psi(t) = \langle\mathbf{u}'(0)\cdot\mathbf{u}'(t)\rangle$ of the fluctuating convection velocity $\mathbf{u}' = \mathbf{u} - \bar{\mathbf{u}}$ varies as

$$\psi(t) = \overline{\mathbf{u}'\cdot\mathbf{u}'} - \frac{u^2\varepsilon\kappa}{k}t + O(t^{3/2}) \qquad (2)$$

as $t\to 0^+$. Equations (1) and (2) are consistent with the preasymptotic dynamics in planar and cylindrical flow [10–19] and imply that the short-time dispersion behavior may be used as a measurement of permeability.

We now turn to a summary of our derivation of the general short-time behavior of $D(t)$ leading to Eq. (1). The term dispersion is used in the context of Taylor's pioneering work [20,21] with regard to ensemble-averaged linear convection-diffusion transport as applied to porous media by Saffman [22]. Formally, the time t-dependent displacement $\mathbf{R}(t) = \mathbf{r}'(t) - \mathbf{r}'(0)$ of a passive particle confined to an equilibrated pore-volume $\boldsymbol{\Omega}$ and driven a steady convection field $\mathbf{u}(\mathbf{r}')$, where $\mathbf{r}' \in \boldsymbol{\Omega}$, is governed by a Langevin stochastic differential equation [1,23]

$$\frac{d}{dt}\mathbf{R}(t) = \mathbf{L}(t) + \mathbf{u}(\mathbf{r}'), \qquad (3)$$

*tyler.brosten@usace.army.mil

where $\mathbf{L}(t)$ is consistent with Brownian motion and a uniform molecular diffusion constant κ. A large particle population is assumed to uniformly saturate the pore-volume. The pore-grain interface is defined by the surface Σ. Over short time and length scales, the convection field varies according to the spatial Taylor series [24]

$$\mathbf{u}(\mathbf{r}') = \mathbf{u}(\mathbf{r}) + \sum_{j=1}^{\infty} \frac{1}{j!}[\mathbf{R}\cdot\nabla]^j \mathbf{u}(\mathbf{r}) \tag{4}$$

where $\mathbf{r} = \mathbf{r}'(0)$. Short-time displacement dynamics resulting from Eq. (3) with the Taylor series Eq. (4) are well known for simple shear and planar flow [10–19], and stationary, homogenous turbulence [24]. In these cases, short-time displacement dynamics resulted from the nonequilibrium interaction of molecular diffusion and spatial variation (stress) of the respective convection field, e.g., velocity gradients. These results suggest the opportunity for permeability measurement through the vector Laplacian of the convection field for small Reynolds number flow through MH porous media [25,26]. Although the exact short-time dynamics are known for Eq. (3) in the special cases of planar and pure shear flow, the exact explicit dynamics are not known for the general three-dimensional Taylor series in Eq. (4).

To address this question, we performed a nonlinear response analysis of the general three-dimensional problem. The derivation is based upon the nonlinear response characteristics of Eq. (3) with the convection expansion Eq. (4). The memoryless components of this system define an input function $\mathbf{h}(t) = \mathbf{u}(\mathbf{r}) + \mathbf{L}(t)$ which drives displacement memory governed by Eq. (4). As a result, we have found the Volterra series [27] to be suited as a representation of displacement

$$\mathbf{R}(t) = \sum_{m=1}^{\infty} \int_0^t d\tau_1 \ldots \int_0^t d\tau_m \mathbf{H}_m(\tau_1,\ldots,\tau_m) : \prod_{k=1}^{m} \mathbf{h}(t-\tau_k). \tag{5}$$

The Volterra kernel matrices $\mathbf{H}_m(\tau_1,\ldots,\tau_m)$ describe displacement response to the static and stochastic input [28]. The kernels are organized by $\mathbf{H}_m = [H_m]_{i=1\ldots n, j=1\ldots n, k=1\ldots n,\ldots}$, where n is the dimensionality, i is the component $\mathbf{R} = [R]_{i=1\ldots n}$, and the entries $j,k,\ldots$ refer to $\mathbf{h}(t-\tau_1) = [h(t-\tau_1)]_{j=1\ldots n}$, $\mathbf{h}(t-\tau_2) = [h(t-\tau_2)]_{k=1\ldots n}$, etc. The Laplace transform of each kernel, $\mathbf{H}_m(s_1,\ldots,s_m)$, describing displacement resulting from Eq. (3) with the convection expansion Eq. (4), was determined using the growing exponential approach [29]. A large s expansion of the kernels leads to the general short-time behavior of $D(t)$ for the pore-saturating fluid particles. A linear mean displacement $\langle\mathbf{R}(t)\rangle = \bar{\mathbf{u}}t$ implies the term varies as

$$D(t) = D_o(t) + D_s(t) + \left(\frac{1}{6}\overline{\mathbf{u}'\cdot\mathbf{u}'} + \frac{1}{3}\kappa\overline{\nabla\cdot\mathbf{u}}\right)t + \left(\begin{array}{l} \frac{1}{6}\overline{\mathbf{u}\cdot(\mathbf{u}\cdot\nabla)\mathbf{u}} + \frac{1}{18}\kappa\overline{\mathbf{u}\cdot\nabla^2\mathbf{u}} + \\ \frac{1}{9}\kappa\overline{\nabla\cdot(\mathbf{u}\cdot\nabla)\mathbf{u}} + \frac{1}{9}\kappa\overline{(\mathbf{u}\cdot\nabla)(\nabla\cdot\mathbf{u})} + \\ \frac{2}{9}\kappa^2\overline{\nabla\cdot\nabla^2\mathbf{u}} + \frac{1}{18}\kappa\overline{\nabla\cdot(\mathbf{I}\cdot\nabla)\mathrm{diag}(\mathbf{u})\mathbf{u}} \end{array}\right)t^2 + O(t^3) \tag{6}$$

as $t\to 0^+$, where $\mathbf{I} = \sum\hat{\mathbf{e}}$ is the sum of standard basis vectors. The nonlinear interaction of convection and diffusion near the pore-grain interface is described by $D_s(t)$. At short times only molecules within the diffusion length $(\kappa t)^{1/2}$ interact with the walls [7,8], implying for a rigid, reflecting, and locally flat pore-grain interface the term varies as

$$D_s(t) = \frac{1}{V_p}\int d\mathbf{r}''\left\{\frac{1}{3}\,\hat{\mathbf{n}}\cdot\mathbf{u}\kappa t + \frac{8}{45\sqrt{\pi}}\hat{\mathbf{n}}\cdot\nabla\,(\hat{\mathbf{n}}\cdot\mathbf{u})(\kappa t)^{3/2} + \left[\frac{1}{6\kappa}\hat{\mathbf{n}}\cdot(\mathbf{u}\cdot\nabla)\mathbf{u} + \frac{1}{12\kappa}\hat{\mathbf{n}}\cdot\nabla(\mathbf{u}\cdot\mathbf{u}) + \frac{1}{6}\hat{\mathbf{n}}\cdot\nabla^2\mathbf{u} + \frac{8}{9}\hat{\mathbf{n}}\cdot\nabla(\nabla\cdot\mathbf{u}) - \frac{13}{18}(\hat{\mathbf{n}}\cdot\nabla)^2(\hat{\mathbf{n}}\cdot\mathbf{u})\right](\kappa t)^2 + O(t^{5/2})\right\} \tag{7}$$

as $t\to 0^+$, where V_p is the integrated pore volume, $\hat{\mathbf{n}}$ is the inward surface normal, and the coefficients are integrated over the pore-grain interface. Surface curvature increases the order of the flat wall terms in powers of $t^{1/2}$.

The generalized terms in Eq. (6) are reduced in the case of Stokes flow for which the Stokes equation, $\nabla p - \mathbf{f} = \mu\nabla^2\mathbf{u}$, and continuity, $\nabla\cdot\mathbf{u} = 0$, govern momentum and mass conservation of the single-phase fluid and a no-slip condition, $\mathbf{u}(\mathbf{r}'')\big|_{r''\in\sum} = 0$, applies at the pore-grain interface. These constraints together with the assumption of a rigid, reflecting, and piecewise smooth pore-grain interface imply $D_s(t)\to O(t^{5/2})$ as $t\to 0^+$. Taken together, these constraints reduce Eq. (6) to

$$D(t) = D_o(t) + \frac{1}{6}\overline{\mathbf{u}'\cdot\mathbf{u}'}t + \left[\frac{1}{6}\overline{\mathbf{u}\cdot(\mathbf{u}\cdot\nabla)\mathbf{u}} + \frac{1}{18}\kappa\overline{\mathbf{u}\cdot\nabla^2\mathbf{u}}\right]t^2 + O(t^{5/2}). \tag{8}$$

Further consider Eq. (8) in the case of a MH porous media for which two volume-average constraints on $\mathbf{u}$ are introduced:

$$\overline{\mathbf{u}\cdot(\mathbf{u}\cdot\nabla)\mathbf{u}} = 0, \tag{9a}$$

$$\overline{\mathbf{u}\cdot\nabla^2\mathbf{u}} = -\varepsilon\bar{\mathbf{u}}\cdot(\mathbf{k}^{-1}\bar{\mathbf{u}}). \tag{9b}$$

The first, Eq. (9a), assumes the ensemble-average convective kinetic energy of the tracer particles is stationary, i.e., on average the fluid does not accelerate. Second, Eq. (9b) follows from substituting the Stokes equation and Darcy's law following volume averaging and is consistent with a homogeneous permeability tensor and fluid volume fraction.

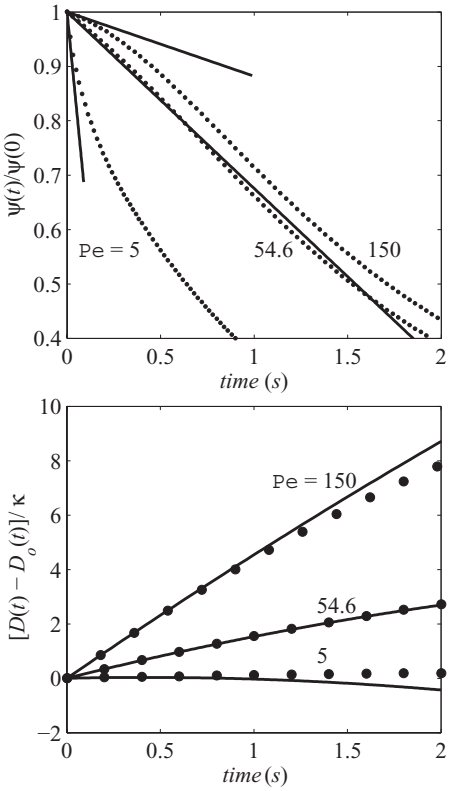

FIG. 1. Analytical short-time predictions compared with numerically simulated hydrodynamic dispersion dynamics in a random sphere pack for three regimes of transport determined by Peclet number. (Top) Comparison of the linear prediction (solid lines) and simulated velocity autocorrelation function (dots). (Bottom) Comparison of the quadratic prediction (solid lines) and simulated difference in effective dispersion and diffusion coefficients (dots). The simulation parameters were $d = 1.0 \times 10^{-4}$ m, $u = 1.0 \times 10^{-5}$ m/s, $\varepsilon = 0.44$, and $k = 1.55 \times 10^{-11}$ m^2.

Thus, Eq. (1) follows from Eqs. (8) and (9) and leads to the connection between short-time dispersion and permeability.

We now demonstrate these results using numerical and PGSE NMR data. A pore-scale Lattice-Boltzmann (LB) simulation [30] of single-phase flow was conducted within a random packing of diameter d monodisperse spheres for Re $= 1 \times 10^{-3}$. The domain consisted of 5^3 spheres and 1024^3 grid points. Fluid viscosity was $\mu/\rho = 1/6$ in lattice units. A pore-saturating population of random-walk particles subject to the steady-state LB-determined velocity field simulated the transient displacement statistics. The computed $\psi(t)$ is compared with the linear prediction from Eq. (2) in the top panel of Fig. 1. The computed $D(t)-D_o(t)$ is compared with the quadratic (two-term) prediction from Eq. (1) in the bottom panel of Fig. 1. The three regimes shown in Fig. 1 are characterized by Peclet number Pe $= ud\varepsilon/[\kappa(1-\varepsilon)]$, where the effective pore length scale $d\varepsilon/(1-\varepsilon)$ is used. Convection-dominated transport is demonstrated by Pe $= 150$, diffusion-dominated transport by Pe $= 5$, and a quasilinear regime of $\psi(t)$ by Pe $= 54.6$. The prediction terms $\overline{\mathbf{u}' \cdot \mathbf{u}'}$ and k were determined from the LB simulation data.

The linear prediction gives excellent agreement with the initial $\psi(t)$ decay for all Pe (top panel of Fig. 1). The convex-to-concave transition in $\psi(t)$ (top panel of Fig. 1) and the corresponding over-to-under transition of the quadratic prediction for $D(t)-D_o(t)$ (bottom panel of Fig. 1) is a product of the three-dimensional pore structure. This transition portends the quasilinear regime of $\psi(t)$ near Pe $= 54.6$ (top panel of Fig. 1); in this regime the quadratic prediction of $D(t)-D_o(t)$ dominates the summation of higher-order terms (bottom panel of Fig. 1).

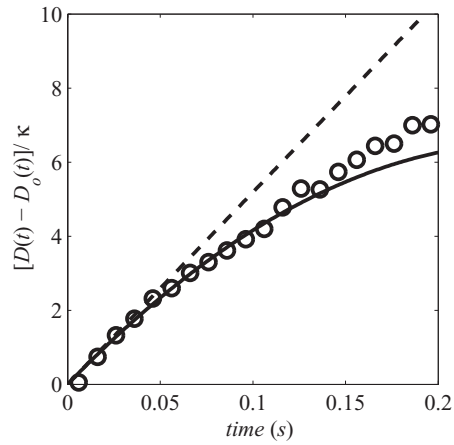

FIG. 2. PGSE NMR measurement of the difference in effective dispersion and diffusion coefficients (open circles) compared with the linear (dashed line) and quadratic (solid line) short-time predictions for Pe $= 50.1$ in a consolidated random sphere pack. Parameters of the experiment were $u = 5.7 \times 10^{-4}$ m/s, Re $= 0.14$, $\varepsilon = 0.42$, $\kappa = 2 \times 10^{-9}$ m^2/s, and $k = 7.4 \times 10^{-11}$ m^2 estimated from the Kozeny-Carman correlation.

The quasilinear regime of $\psi(t)$ is further demonstrated in Fig. 2 by PGSE NMR data for Pe $= 50.1$. Previously, PGSE NMR has been used to characterize transient dispersion dynamics in porous media in the ideal sense that the fluid molecules themselves act as the tracer particles [31–35]. The data in Fig. 2 characterizes $D(t)-D_o(t)$ of water fully saturating a packed bed of $d = 240$ μm polystyrene spheres (Duke Scientific) within a 10-mm-diam glass capillary. Also shown in Fig. 2 are the linear and quadratic short-time predictions of $D(t)-D_o(t)$ from Eq. (1). The dynamics were measured using a stimulated echo single PGSE sequence implemented on a Bruker 300-MHz superconducting magnet interfaced to a Micro2.5 gradient probe. The gradient of the PGSE sequence was incremented through eight values along three orthogonal axes for each observation time with and without steady flow driven by a Pharmacia P500 high-pressure liquid chromatography pump. The total coefficients $D(t)$ and $D_o(t)$ were determined by averaging the respective orthogonal coefficients from the Stejskal-Tanner relation for the NMR signal intensity [36].

The PGSE NMR data shown in Fig. 2 is a Peclet number regime in which neither convection nor molecular diffusion dominate molecular displacement. Agreement between the quadratic short-time prediction (solid line) and data is excellent. Transitioning the Peclet number to a more diffusion- or convection-dominated regime necessitates the inclusion of higher-order (greater than t^2) expansion terms to maintain the short-time prediction accuracy (see Fig. 1). The linear short-time prediction (dashed line) coefficient in Fig. 2 was estimated

from a linear fit to initial data points. Permeability k entering the t^2 coefficient of the quadratic prediction was estimated by the Kozeny-Carman correlation $k = d^2\varepsilon^3/[180(1-\varepsilon)^2]$ [2] because the packed bed confinement mechanism prevented an accurate classic measurement of permeability; the correlation predicts the LB-simulated permeability within 2.7%. Fluid volume fraction ε was determined by comparing the measured intrinsic average and superficial flow velocities. The excellent agreement in Fig. 2 between data and short-time quadratic prediction indicates a measurement of permeability by postprocessing PGSE NMR measurement of the short-time dynamics.

A general short-time expansion of the effective dispersion coefficient for steady flow and Brownian fluid particles was interpreted in terms of Stokes flow through MH porous media with a piecewise smooth pore-grain interface. The result facilitates a noninvasive measurement of hydrodynamic permeability by postprocessing PGSE NMR measurement of the effective dispersion coefficient. A virtue of this technique is that it does not require knowledge of the pressure gradient nor fluid viscosity. The general short-time expansion suggests a broader interpretation and application of stochastic hydrodynamic dispersion dynamics for inertial, multiphase, electro-osmotic, non-Newtonian, and other flows.

[1] H. Brenner and D. A. Edwards, *Macrotransport Processes* (Butterworth-Heinemann, Boston, 1993).
[2] J. Bear, *Dynamics of Fluids in Porous Media* (Elsevier, New York, 1972).
[3] F. A. L. Dullien, *Porous Media; Fluid Transport and Pore Structure* (Academic, New York, 1979).
[4] M. Sahimi, Rev. Mod. Phys. **65**, 1393 (1993).
[5] Y. A. Urzhumov and D. R. Smith, Phys. Rev. Lett. **107**, 074501 (2011).
[6] S. Vogel, *Life in Moving Fluids: The Physical Biology of Flow* (Princeton University Press, Princeton, NJ, 1996).
[7] P. P. Mitra, P. N. Sen, L. M. Schwartz, and P. Le Doussal, Phys. Rev. Lett. **68**, 3555 (1992).
[8] P. P. Mitra, P. N. Sen, and L. M. Schwartz, Phys. Rev. B **47**, 8565 (1993).
[9] J. P. Boon and S. Yip, *Molecular Hydrodynamics* (McGraw Hill, New York, 1980).
[10] M. J. Lighthill, IMA J. Appl. Math. **2**, 97 (1966).
[11] P. C. Chatwin, J. Fluid Mech. **43**, (1970).
[12] R. T. Foister and T. G. M. Van de Ven, J. Fluid Mech. **96**, (1980).
[13] C. Van den Broeck, Physica A **112**, 352 (1982).
[14] N. Liron and J. Rubinstein, SIAM J. Appl. Math. **44**, 493 (1984).
[15] W. R. Young and S. Jones, Phys. Fluids A **3**, 1087 (1991).
[16] P. T. Callaghan, S. L. Codd, and J. D. Seymour, Conc. Magn. Res. **11**, 181 (1999).
[17] R. Camassa, Z. Lin, and R. M. McLaughlin, Commun. Math. Sci. **8**, 601 (2010).
[18] R. Camassa, R. M. McLaughlin, and C. Viotti, Phys. Fluids **22**, 117103 (2010).
[19] R. R. Ratnakar and V. Balakotaiah, Phys. Fluids **23**, (2011).
[20] G. I. Taylor, Proc. R. Soc. London **219**, 186 (1953).
[21] R. Aris, Proc. R. Soc. London **235**, 67 (1956).
[22] P. G. Saffman, J. Fluid Mech. **6**, 321 (1959).
[23] N. G. Van Kampen, *Stochastic Processes in Physics and Chemistry* (Elsevier, Oxford, 2007).
[24] P. G. Saffman, J. Fluid Mech. **8**, 273 (1960).
[25] J. C. Slattery, AIChE J. **13**, 1066 (1967).
[26] S. Whitaker, Transp. Porous Media **1**, 3 (1986).
[27] V. Volterra, *Theory of Functionals and of Integral and Integro-differential Equations* (Dover, New York, 1959).
[28] N. Wiener, *Nonlinear Problems in Random Theory* (The MIT Press, Cambridge, MA, 1966).
[29] W. J. Rugh, *Nonlinear System Theory: The Volterra/Wiener Approach* (Johns Hopkins University Press, Baltimore, 1981).
[30] R. S. Maier, D. M. Kroll, R. S. Bernard, S. E. Howington, J. F. Peters, and H. T. Davis, Phys. Fluids **12**, 2065 (2000).
[31] J. D. Seymour and P. T. Callaghan, AIChE J. **43**, 2096 (1997).
[32] B. Manz, L. F. Gladden, and P. B. Warren, AIChE J. **45**, 1845 (1999).
[33] U. M. Scheven and P. N. Sen, Phys. Rev. Lett. **89**, 254501 (2002).
[34] U. M. Scheven, R. Harris, and M. L. Johns, Phys. Rev. Lett. **99**, 054502 (2007).
[35] T. R. Brosten, S. L. Codd, R. S. Maier, and J. D. Seymour, Phys. Rev. Lett. **103**, 218001 (2009).
[36] P. T. Callaghan, *Principles of Nuclear Magnetic Resonance Microscopy* (Oxford University Press, Oxford, UK, 1991).